Preparation, Stereochemistry, and Reactivity of Linear-Type S-Bridged $MCr^{III}M$ ($M=Rh^{III}$, Ir^{III}) Trinuclear Complexes with 2-Aminoethanethiolate (aet). Crystal Structures of $\Delta\Lambda$-$[Cr\{M(aet)_3\}_2]^{3+}$

Yoshitaro Miyashita, Narumi Sakagami, Yasunori Yamada, Takumi Konno,† Jinsai Hidaka,†† and Ken-ichi Okamoto*

Department of Chemistry, University of Tsukuba, Tsukuba, Ibaraki 305

†Department of Chemistry, Faculty of Engineering, Gunma University, Kiryu, Gunma 376

††Department of Industrial Chemistry, Faculty of Engineering, Kinki University in Kyushu, Iizuka, Fukuoka 820

(Received October 27, 1997)

S-Bridged trinuclear complexes, $[Cr^{III}\{M(aet)_3\}_2]^{3+}$, ($M=Rh^{III}$ (**1**), Ir^{III} (**2**); aet = $NH_2CH_2CH_2S^-$) were newly prepared by the reaction of *fac*(*S*)-$[M(aet)_3]$ with chromium(III) nitrate. They were separated and optically resolved into the $\Delta\Delta$, $\Lambda\Lambda$, and $\Delta\Lambda$ isomers. Of these isomers for **1** and **2**, the crystal structures of the $\Delta\Lambda$ isomers (**1a** and **2a**) were determined by an X-ray diffraction method. Each of **1a** and **2a** consists of two *fac*(*S*)-$[M(aet)_3]$ subunits, a central Cr atom, three nitrates, and three water molecules, $[Cr\{M(aet)_3\}_2](NO_3)_3\cdot 3H_2O$, in which three metals are aligned so as to be exactly linear. The central Cr atom is situated in an octahedral environment with the $Cr^{III}S_6$ chromophore, which is formed by the coordination of two terminal *fac*(*S*)-$[M(aet)_3]$ units. The other isomers for **1** and **2** were characterized by the absorption and CD spectra, the molar conductivity, and the magnetic susceptibility. Each cyclic voltammogram of $\Delta\Lambda$-$[Cr\{M(aet)_3\}_2]^{3+}$ in water showed a reversible redox couple (M(IV)/M(III)) and an irreversible reduction wave (Cr(III)/Cr(II)). The stabilities of the S-bridged $MCr^{III}M$ complexes are also discussed in relation to the Cr–S bond strengths.

We have reported that the formation of the S-bridged polynuclear structures are highly dependent on the coordination geometry of the reacting metal ions. Namely, the mononuclear complexes, *fac*(*S*)-$[M(aet)_3]$ ($M=Co^{III}$, Rh^{III}, Ir^{III}; aet = $NH_2CH_2CH_2S^-$), function as tridentate ligands, and the reactions with metal ions (M′), which prefer to take the octahedral coordination geometry, produce linear-type S-bridged trinuclear complexes, $[M'\{M(aet)_3\}_2]^{n+}$.[1—12] The Cr(III) ion tends to take an octahedral geometry and it will be expected to form a similar trinuclear structure. However, the Cr–S bond-cleavage reactions in $[Cr(\text{L-cys-}N,O,S)_2]^-$ have been widely recognized[13—15] in terms of a strong affinity for oxygen atoms and a relatively weak affinity for sulfur atoms. Further, although S-bridged polynuclear Cr(III) complexes with a soft sulfur donor ligand, which has the $Cr^{III}S_6$ chromophore, have been little known, they are of interest in connection with their stereochemical, spectrochemical and magnetic features. Accordingly, it is worth attempting a reaction of the Cr(III) ion with *fac*(*S*)-$[M(aet)_3]$ ($M=Rh^{III}$, Ir^{III}) in order to elucidate the reactivity of the Cr(III) ion toward metal complexes with sulfur donor atoms as well as the fundamental properties of the Cr(III) ion incorporated in the polynuclear structures. In the present paper, we report that linear-type S-bridged trinuclear complexes, $[Cr\{M(aet)_3\}_2]^{3+}$ ($M=Rh^{III}$ (**1**); Ir^{III} (**2**)), were prepared, separated, and optically resolved into possible isomers. These isomers for **1** and **2** were mainly characterized by the absorption and CD spectra, and the representative crystal structures of $\Delta\Lambda$-$[Cr\{M(aet)_3\}_2]^{3+}$ were determined by an X-ray diffraction study. The stereochemical, spectrochemical, and electrochemical behavior for the present complexes and the reactivity around the Cr(III) ion in these systems are also discussed.

Experimental

Materials. 2-Aminoethanethiol (Haet) was purchased from Tokyo Kasei Organic Chemical Co., Inc. $RhCl_3\cdot nH_2O$ and $IrCl_3$ were purchased from N. E. Chemcat Co., Ltd., and Rare Metallic Co., Ltd., respectively. $Na_2[Sb_2(d\text{-tartrato})_2]\cdot 5H_2O$ was prepared from $Na(d\text{-}H_3\text{tartrato})\cdot H_2O$ and Sb_2O_3. The other reagents were obtained from Wako Pure Chemical Ind., Co., Ltd. All of the chemicals were of reagent grade and used without further purification.

Preparation and Resolution of Complexes. ***fac*(*S*)-$[Rh(aet)_3]$.** This complex was prepared by a modified method from the literature.[16,17] A solution containing 7.61 g (98.6 mmol) of Haet in 40 cm^3 of water was added to a solution containing 3.95 g (98.8 mmol) of NaOH in 40 cm^3 of water. To this was added 2.46 g (9.56 mmol) of $RhCl_3\cdot nH_2O$. The mixture was stirred under a nitrogen atmosphere while gradually raising the temperature to 95—100 °C for 30 min, and then further stirred at 95—100 °C for 3.5 h. After cooling to room temperature, the resulting yellow precipitate was collected by filtration and washed with a large amount of water and methanol. Yield: 2.63 g (83.0%).

***fac*(*S*)-[Ir(aet)$_3$].** This complex was prepared by a modified method of Konno et al.[11] To a solution containing 8.36 g (209 mmol) of NaOH in 150 cm^3 of water was added 15.41 g (200 mmol) of Haet. To this was added 3.00 g (10.1 mmol) of $IrCl_3$. The mixture was stirred under a nitrogen atmosphere while gradually raising the temperature to 110—115 °C for 45 min, and further stirred at 110—115 °C for 3 d. After cooling to room temperature, the resulting off-white precipitate was collected by filtration and washed with a large amount of water and methanol. To the rough powder was added 100 cm^3 of a 1 mol dm^{-3} HCl solution, and insoluble dark-gray materials were removed by filtration. The pale-brown solution was neutralized with a 6 mol dm^{-3} NaOH solution. The resulting pale-yellow-green precipitate was collected by filtration and washed with a large amount of water and methanol. Yield: 2.28 g (53.9%).

[Cr{Rh(aet)$_3$}$_2$]$^{3+}$ (1). To a suspension containing 0.30 g (0.91 mmol) of *fac*(*S*)-[Rh(aet)$_3$] in 10 cm^3 of water was added 2.00 g (5.00 mmol) of $Cr(NO_3)_3\cdot 9H_2O$. The mixture was stirred at 60 °C for 1 h, whereupon it became a dark-brown solution. The solution was left standing at room temperature for 1 h. The resulting black plate crystals (**1a**$(NO_3)_3\cdot 3H_2O$) were collected by filtration and washed with a small amount of acetone. Yield: 0.17 g. **1a**$(NO_3)_3\cdot 3H_2O$ was recrystallized from warm water by adding one drop of a saturated $NaNO_3$ solution. Found: C, 14.82; H, 4.66; N, 12.88; Cr, 5.36; Rh, 21.49%. Calcd for $[Cr\{Rh(aet)_3\}_2](NO_3)_3\cdot 3H_2O = C_{12}H_{36}O_9N_9S_6CrRh_2\cdot 3H_2O$: C, 15.10; H, 4.43; N, 13.20; Cr, 5.45; Rh, 21.56%.

After removing **1a**$(NO_3)_3\cdot 3H_2O$ by filtration, to the filtrate was added ca. 5 cm^3 of a saturated NaBr solution, followed by keeping in a refrigerator for 1 d. The resulting black needle crystals (**1b**$Br_3\cdot 1.5H_2O$) were collected by filtration and washed with a small amount of acetone. Yield: 0.13 g. **1b**$Br_3\cdot 1.5H_2O$ was recrystallized from warm water by adding one drop of a saturated NaBr solution. Found: C, 14.75; H, 4.01; N, 8.67; Cr, 5.12; Rh, 21.07%. Calcd for $[Cr\{Rh(aet)_3\}_2]Br_3\cdot 1.5H_2O = C_{12}H_{36}N_6S_6Br_3CrRh_2\cdot 1.5H_2O$: C, 14.69; H, 4.01; N, 8.56; Cr, 5.30; Rh, 20.97%.

1a and **1b** were also separated by an SP-Sephadex C-25 column chromatography apparatus. Three bands (black (excess Cr^{3+}), orange (**1a**), and brown (**1b**)) were eluted in this order with a 0.3 mol dm^{-3} NaCl solution. The brown eluate **1b** was charged on the top of the SP-Sephadex C-25 column. Two bands, $(-)^{\mathrm{CD}}_{600}$-**1b** and $(+)^{\mathrm{CD}}_{600}$-**1b**, were separated by eluting with a 0.1 mol dm^{-3} $Na_2[Sb_2(d\text{-tart})_2]\cdot 5H_2O$ aqueous solution. After the two bands were completely separated, the $(-)^{\mathrm{CD}}_{600}$-**1b** and $(+)^{\mathrm{CD}}_{600}$-**1b** isomers were eluted with a 0.3 mol dm^{-3} NaCl solution. **1a** was not optically resolved by the same method. The $\Delta\varepsilon$ values of each eluate containing the $(-)^{\mathrm{CD}}_{600}$-**1b** and $(+)^{\mathrm{CD}}_{600}$-**1b** isomers were evaluated on the basis of the absorption spectral data of **1b**$Br_3\cdot 1.5H_2O$.

[Cr{Ir(aet)$_3$}$_2$]$^{3+}$ (2). To a suspension containing 0.30 g (0.71 mmol) of *fac*(*S*)-[Ir(aet)$_3$] in 7 cm^3 of water was added 2.00 g (5.00 mmol) of $Cr(NO_3)_3\cdot 9H_2O$. The mixture was stirred at 60 °C for 10 min, whereupon it became a dark-brown solution. The solution was left standing at room temperature for 1 h. The resulting black plate crystals (**2a**$(NO_3)_3\cdot 3H_2O$) were collected by filtration and washed with a small amount of acetone. Yield: 0.15 g. **2a**$(NO_3)_3\cdot 3H_2O$ was recrystallized from warm water by adding a few drops of a saturated $NaNO_3$ solution. Found: C, 12.46; H, 3.82; N, 10.84; Cr, 4.32; Ir, 33.70%. Calcd for $[Cr\{Ir(aet)_3\}_2](NO_3)_3\cdot 3H_2O = C_{12}H_{36}O_9N_9S_6CrIr_2\cdot 3H_2O$: C, 12.71; H, 3.74; N, 11.12; Cr, 4.59; Ir, 33.92%.

After removing **2a**$(NO_3)_3\cdot 3H_2O$ by filtration, to the filtrate was added ca. 3 cm^3 of a saturated NaBr solution, followed by keeping in a refrigerator for 3 h. The resulting black needle crystals (**2b**$Br_3\cdot 1.5H_2O$) were collected by filtration and washed with a small amount of acetone. Yield: 0.12 g. **2b**$Br_3\cdot 1.5H_2O$ was recrystallized from warm water by adding a few drops of a saturated NaBr solution. Found: C, 12.52; H, 3.50; N, 7.26; Cr, 4.06; Ir, 33.81%. Calcd for $[Cr\{Ir(aet)_3\}_2]Br_3\cdot 1.5H_2O = C_{12}H_{36}N_6S_6Br_3CrIr_2\cdot 1.5H_2O$: C, 12.42; H, 3.39; N, 7.24; Cr, 4.48; Ir, 33.14%.

2a and **2b** were also separated by a column chromatographic treatment similar to that used for **1**. Three bands (black (excess Cr^{3+}), brown (**2a**), and brown (**2b**)) were eluted in this order using a 0.3 mol dm^{-3} NaCl solution. The brown eluate **2b** was charged on the top of the SP-Sephadex C-25 column. Two bands, $(-)^{\mathrm{CD}}_{600}$-**2b** and $(+)^{\mathrm{CD}}_{600}$-**2b**, were partially separated by eluting with a 0.1 mol dm^{-3} $Na_2[Sb_2(d\text{-tart})_2]\cdot 5H_2O$ aqueous solution. The pure $(-)^{\mathrm{CD}}_{600}$-**2b** and $(+)^{\mathrm{CD}}_{600}$-**2b** parts, which were found by absorption and CD measurements, were eluted and fractionated with a 0.3 mol dm^{-3} NaCl solution. **2a** was not optically resolved by the same method. The $\Delta\varepsilon$ values of each band of the $(-)^{\mathrm{CD}}_{600}$-**2b** and $(+)^{\mathrm{CD}}_{600}$-**2b** isomers were evaluated on the basis of the absorption spectral data of **2b**$Br_3\cdot 1.5H_2O$.

Measurement. The electronic absorption spectra were recorded with JASCO UVIDEC-505, Ubest-55, and V-560 spectrophotometers. The CD spectra were recorded with a JASCO J-600 spectropolarimeter. All of the measurements were carried out in aqueous solutions at room temperature. The elemental analyses (C, H, N) were performed by the Analysis Center of the University of Tsukuba. The concentrations of Cr, Rh, and Ir in the complexes were determined with a NIPPON Jarrell-Ash ICPA-575 ICP spectrophotometer. The molar conductance of the complexes were measured with a Horiba conductivity meter (DS-14) in aqueous solutions at room temperature. The magnetic measurements were performed by using a Sherwood Scientific apparatus at 23 °C. Electrochemical measurements were performed by a CV-1B apparatus (Biochemical Systems, Inc. (BSI)) using a glassy-carbon working electrode (BSI). An aqueous Ag/AgCl/NaCl (3 mol dm^{-3}) electrode (BSI) and platinum wire were used as reference and auxiliary electrodes, respectively. The electrochemical experiments were conducted by the complex concentrations of 1.0 mmol dm^{-3} in a 0.1 mol dm^{-3} aqueous solution of Na_2SO_4 as the supporting electrolyte. The changes with times were carried out by absorption spectral measurements and the column chromatographic technique. A solution containing 0.02 g of *meso*-$[Cr\{Ir(aet)_3\}_2](NO_3)_3\cdot 3H_2O$ in 25 cm^3 of 1 mol dm^{-3} HCl solution was maintained at 40 °C for a definite time. Using 5 cm^3 of these solutions, which was diluted to 25 cm^3 by a 1 mol dm^{-3} HCl solution, the absorption spectral changes with times were measured on a JASCO V-560 spectrophotometer. Another solution of 20 cm^3 was poured onto the SP-Sephadex C-25 column and eluted by a 1 mol dm^{-3} NaCl solution. Each eluate was diluted to 100 cm^3 and its concentration was measured on a JASCO V-560 spectrophotometer.

Crystallography. A single crystal of **1a**$(NO_3)_3\cdot 3H_2O$ or **2a**$(NO_3)_3\cdot 3H_2O$ was used for data collection on an Enraf Nonius CAD4 diffractometer with graphite-monochromatized Mo $K\alpha$ (0.71073 Å) radiation. The unit-cell parameters were determined by a least-squares refinement of 25 reflections. The crystal data and experimental parameters are listed in Table 1. The intensity data were collected by the ω–2θ scan technique, and the scan rate varied from 1 to 5° min^{-1} (on ω). The intensities were corrected for Lorentz and polarization. An empirical absorption correction based on a series of Ψ scans was applied. Independent reflections

Table 1. Crystal Data for $[Cr\{M(aet)_3\}_2](NO_3)_3\cdot 3H_2O$ ($M = Rh^{III}$, **1a**; Ir^{III}, **2a**)

	1a	**2a**
Formula	$C_{12}H_{42}N_9O_{12}S_6CrRh_2$	$C_{12}H_{42}N_9O_{12}S_6CrIr_2$
Formula weight	954.68	1133.31
Cryst. system	Triclinic	Triclinic
Space group	$P\bar{1}$	$P\bar{1}$
a/Å	8.9088(7)	8.904(2)
b/Å	8.9347(7)	8.942(2)
c/Å	12.149(1)	12.136(2)
α/°	71.133(7)	70.69(2)
β/°	70.228(5)	70.20(2)
γ/°	77.680(6)	77.56(2)
V/Å^3	855.3(1)	852.1(4)
Z	1	1
D_{calcd}/g cm^{-3}	1.85	2.208
Cryst. dimems./mm	$0.25\times0.18\times0.09$	$0.18\times0.12\times0.08$
μ(Mo $K\alpha$)/mm^{-1}	1.69	8.55
Transm. Coeff.	0.803—0.999	0.789—0.998
Temp/K	296	296
λ (Mo $K\alpha$)/Å	0.71073	0.71073
No. of measd reflcns	4990	3021
No. of reflcns for used	3851	2783
No. of parameters	250	232
Final R	0.039	0.032
Final R_w	0.048	0.040
GOF	1.29	1.26

with $I_0 > 1.5\ \sigma(I_0)$ were used for structure determinations.

The atomic positions of Rh or Ir, Cr, and other non-hydrogen atoms were determined by a direct method. The structures were refined by a full-matrix least-squares refinement on F of the positional parameters and the anisotropic thermal parameters of the non-hydrogen atoms in **1a**$(NO_3)_3\cdot 3H_2O$ or **2b**$(NO_3)_3\cdot 3H_2O$. The hydrogen atoms on the aet ligands were fixed by the geometrical and thermal constrains (C–H=N–H=0.95 Å and $U=1.3U$(C)). The occupancy factors (occ) for some atoms are listed in Tables 2 and 3. All of the calculations were performed on a Indigo II computer using teXsan.[18] The final atomic coordinates for non-hydrogen atoms are also given in Tables 2 and 3.[19]

Results and Discussion

X-Ray Crystal Structures of 1a and 2a. Perspective drawings of the entire complex cations, **1a** and **2a**, are given in Figs. 1 and 2. The selected bond distances and angles are listed in Tables 4 and 5. The complex cations, **1a** and **2a**, consist of two approximately octahedral *fac*(*S*)-$[M(aet)_3]$ ($M = Rh^{III}$ (**1a**); Ir^{III} (**2a**)) units and one Cr atom. These are consistent with the results of a plasma emission spectral analysis, which gave a value of Cr : M = 1 : 2. The three thiolato sulfur atoms in each *fac*(*S*)-$[M(aet)_3]$ unit coordinate to the central Cr atom, forming the $Cr^{III}S_6$ chromophore. The crystallographic inversion center locates at the Cr atom, and requires that the three metals are aligned to be exactly linear (Tables 4 and 5). These, therefore, indicate that **1a** and **2a** complete linear-type S-bridged MCrM trinuclear structures, $[Cr^{III}\{M(aet)_3\}_2]^{3+}$.

The coordination geometry of the central Cr atom in $[Cr\{M(aet)_3\}_2]^{3+}$ is trigonally distorted from a regular octahedron, which has the acute S–Cr–S bite angles (av. 83.69(3)° for **1a**; 84.36(6)° for **2a**) for the ligating *fac*(*S*)-$[M(aet)_3]$ unit. For the terminal *fac*(*S*)-$[M(aet)_3]$ units, the S_3 faces are compressed to give acute S–M–S angles (av. 87.63(3)° for **1a**; 88.45(6)° for **2a**), while the N_3 faces are expanded to give obtuse N–M–N angles (av. 95.5(1)° for **1a**; 95.1(2)° for **2a**). These angles seem to be affected by the sizes for the central and terminal metal ions.[6,10—12] It is noted that the Ir–Cr distances (2.9096(3) Å) in **2a** are somewhat shorter (0.0232 Å) than the corresponding Rh–Cr ones (2.9328(2) Å) in **1a**, although the Cr–S (av. 2.421(2) Å) and Ir–S (av. 2.330(2) Å) distances for **2a** are longer than the corresponding Cr–S (av. 2.4110(8) Å) and Rh–S (av. 2.3232(8) Å) ones for **1a**, respectively. This corresponds with the facts that the bridging Ir–S–Cr bite angles (av. 75.51(5)°) are more acute than the corresponding Rh–S–Cr ones (av. 76.53(2)°).

The overall structure of **2a** is fairly similar to that of the corresponding $[Co\{Ir(aet)_3\}_2]^{3+}$.[11] However, the Cr–S distance (av. 2.421(2) Å) is ca. 0.16 Å longer than the corresponding Co–S distance (av. 2.262(11) Å). This fact is in agreement with the results that the Cr–S distances of $[Cr(C_2H_5SCS_2)_3]$ (av. 2.400(1) Å) and $[Ni\{Cr(aet)_3\}_2]^{2+}$ (av. 2.370(2) Å) are ca. 0.1 Å longer than the Co–S distances of $[Co(C_2H_5SCS_2)_3]$ (av. 2.272(1) Å) and $[Ni\{Co(aet)_3\}_2]^{2+}$ (av. 2.253(1) Å), respectively,[10,20,21] reflecting the larger size of the $Cr^{III}S_6$ chromophore than that of the $Co^{III}S_6$ chromophore. Further, the Cr–S distances of $[Cr\{Rh(aet)_3\}_2]^{3+}$ (av. 2.4110(8) Å) and $[Cr\{Ir(aet)_3\}_2]^{3+}$ (av. 2.421(2) Å) are ca. 0.04 Å longer than those of $[Ni\{Cr(aet)_3\}_2]^{2+}$ (av. 2.370(2) Å),[21] in which the Cr atoms locate in the terminal *fac*(*S*)-$[Cr(aet)_3]$ units. The Cr atoms in $[Cr\{M(aet)_3\}_2]^{3+}$ has the CrS_6 chromophore and six coordinated S atoms

Table 2. Final Atomic Coordinates, Equivalent Thermal Parameters (B_{eq}/Å^2), and Occupancy Factors (occ) for Non-Hydrogen Atoms of [Cr{Rh(aet)$_3$}$_2$](NO$_3$)$_3$·3H$_2$O (**1a**) ($B_{eq} = (8\pi^2/3)\Sigma\Sigma U_{ij}a_i^* a_j^* \mathbf{a}_i\cdot\mathbf{a}_j$)

Atom	x	y	z	B_{eq}	Occ
Rh(1)	0.22545(3)	0.14405(3)	0.76707(2)	2.334(4)	
Cr(1)	0.0000	0.0000	1.0000	2.34(1)	1/2
S(1)	−0.03120(9)	0.25264(9)	0.85463(7)	2.81(1)	
S(2)	0.12006(9)	−0.09482(9)	0.81968(6)	2.73(1)	
S(3)	0.26726(9)	0.06086(9)	0.95762(7)	2.81(1)	
N(1)	0.2955(3)	0.3694(3)	0.7337(2)	3.59(6)	
N(2)	0.1716(3)	0.1974(3)	0.6016(2)	3.27(5)	
N(3)	0.4609(3)	0.0320(3)	0.7058(2)	3.28(5)	
C(1)	0.0354(5)	0.4115(4)	0.8842(3)	4.09(7)	
C(2)	0.1601(5)	0.4880(4)	0.7704(4)	4.68(8)	
C(3)	0.0081(4)	−0.0260(4)	0.7078(3)	3.71(6)	
C(4)	0.1184(4)	0.0580(5)	0.5881(3)	4.02(7)	
C(5)	0.4176(4)	−0.1064(4)	0.9252(3)	3.58(6)	
C(6)	0.5387(4)	−0.0420(5)	0.8048(3)	3.98(7)	
N(4)	0.7441(4)	0.3424(4)	0.5541(3)	4.85(7)	
N(5)	0.493(1)	0.518(1)	0.123(2)	14.7(4)	1/2
O(1)	0.7570(8)	0.1992(7)	0.5829(7)	8.9(2)	2/3
O(2)	0.8552(6)	0.4052(8)	0.5416(7)	7.6(1)	2/3
O(3)	0.6231(6)	0.4162(7)	0.5213(4)	6.7(1)	2/3
O(4)	0.698(2)	0.270(2)	0.511(1)	8.8(3)	1/3
O(5)	0.688(2)	0.277(2)	0.679(1)	8.6(3)	1/3
O(6)	0.835(2)	0.443(1)	0.528(1)	11.6(3)	1/3
O(7)	0.615(1)	0.538(1)	0.023(1)	11.7(3)	1/2
O(8)	0.402(1)	0.4775(10)	0.0478(7)	7.3(2)	1/2
O(9)	0.428(1)	0.545(2)	0.1889(8)	6.5(2)	1/4
O(10)	0.470(1)	0.519(2)	0.2057(8)	6.8(2)	1/4
O(1w)	0.1906(10)	0.3602(8)	0.3082(6)	7.3(2)	1/2
O(2w)	0.5100(4)	−0.2456(4)	0.5973(3)	5.33(7)	

are, of course, *trans* to other S atoms. However, the Cr atoms in [Ni{Cr(aet)$_3$}$_2$]$^{2+}$ have the CrN$_3$S$_3$ chromophore, and three coordinated S atoms have mutually *cis* positions. This means that the Cr–S distances which occupy the *trans* position to the S atom are longer than those to the other N or O atom. A similar trend was also observed; that is, the Cr–S distances that occupy the *trans* position to the S atom are 2.400(1) Å in [Cr(C$_2$H$_5$SCS$_2$)$_3$],[20] 2.416(1) Å in *trans*(*S*)-[Cr(L-cys-*N*,*O*,*S*)$_3$]$^-$,[22] 2.389(5) Å in *trans*(*S*)-[Cr(aet)$_2$(en)]$^+$,[23] and 2.396(7) Å in [Cr(C$_2$O$_2$S$_2$)$_3$(NiL)$_3$]$^{3+}$ (L = *racemi*-5,5,7,12,12,14-hexamethyl-1,4,8,11-tetraazacyclotetradecane).[24] On the other hand, the Cr–S distances that occupy the *trans* position to the O or N atom are 2.337(2) Å in [Cr(SCH$_2$CH$_2$COO)(en)$_2$]$^+$ [25] and 2.332(2) Å in [Cr(L-his)-(D-pen)] (L-his = L-histidine, D-pen = D-penicillaminate),[26] and 2.364(5) Å in [Cr{Cr(SCH$_2$CH$_2$O)$_3$}$_2$]$^{3-}$.[27] Accordingly, the Cr–S bond lengthening of [Cr{M(aet)$_3$}$_2$]$^{3+}$, compared with [Ni{Cr(aet)$_3$}$_2$]$^{2+}$, would be due to the sulfur trans influence.

Considering the absolute configurations (*Δ* and *Λ*) of the two terminal *fac*(*S*)-[M(aet)$_3$] (M = Rh^{III}, Ir^{III}) units, three isomers (*ΔΔ*, *ΛΛ*, and *ΔΛ*), are possible for the present trinuclear complexes, [Cr{M(aet)$_3$}$_2$]$^{3+}$. The space group $P\bar{1}$ and $Z = 1$ clearly indicates that **1a** and **2a** are a *meso* isomer containing the *Δ*- and *Λ*-*fac*(*S*)-[M(aet)$_3$] units, as shown in Figs. 1 and 2. This is consistent with the fact that **1a** and **2a** were not optically resolved. The aet chelate rings have a distinct *gauche* form with the *λ* conformation for the *Δ*-*fac*(*S*)-[M(aet)$_3$] unit and the *δ* conformation for the *Λ* unit. Therefore, all of the bridging sulfur atoms are fixed to the *R* configuration for the *Δ*-*fac*(*S*)-[M(aet)$_3$] unit and the *S* configuration for the *Λ* unit. The stereochemical behavior are wholly consistent with that observed in the corresponding trinuclear complexes.[6,10—12]

Characterization. The electronic absorption and CD spectra of **1a**, $(-)^{CD}_{600}$-**1b**, **2a**, and $(-)^{CD}_{600}$-**2b** are shown in Figs. 3 and 4. The data are summarized in Table 6. The absorption spectrum of **1b** is quite similar to that of *ΔΛ*-[Cr{Rh(aet)$_3$}$_2$]$^{3+}$ (**1a**), whose structure was determined by an X-ray crystal analysis over the whole region, although the intensity of the bands at 16 and 25×10^3 cm^{-1} for **1b** slightly differs from those for **1a**. Similarly, the absorption spectrum of **2b** agrees well with that of *ΔΛ*-[Cr{Ir(aet)$_3$}$_2$]$^{3+}$ (**2a**). The elemental analytical data for **1b** and **2b** as well as those for **1a** and **2a** are in good agreement with the proposed formula, [Cr{M(aet)$_3$}$_2$]$^{3+}$ (M = Rh^{III} (**1**) and Ir^{III} (**2**)). The plasma emission spectral analyses for **1b** and **2b** also indicate that the ratio of Cr : M is 1 : 2. Furthermore, **1b** and **2b** were optically resolved into the $(-)^{CD}_{600}$ and $(+)^{CD}_{600}$ isomers, which exhibit enantiomeric CD spectra to each other. Accordingly, these facts indicate that **1b** and **2b** are also geometrical isomers of the trinuclear complexes, that is, **1b** or **2b** is the

Table 3. Final Atomic Coordinates, Equivalent Thermal Parameters (B_{eq}/Å^2), and Occupancy Factors (Occ) for Non-Hydrogen Atoms of $[Cr\{Ir(aet)_3\}_2](NO_3)_3 \cdot 3H_2O$ (**2a**) ($B_{eq} = (8\pi^2/3)\Sigma\Sigma U_{ij} a_i^* a_j^* \boldsymbol{a}_i \cdot \boldsymbol{a}_j$)

Atom	x	y	z	B_{eq}	Occ
Ir(1)	0.22384(3)	0.14426(3)	0.76807(2)	2.175(6)	
Cr(1)	0.0000	0.0000	1.0000	2.22(3)	1/2
S(1)	−0.0335(2)	0.2558(2)	0.8543(2)	2.67(3)	
S(2)	0.1194(2)	−0.0957(2)	0.8193(2)	2.59(3)	
S(3)	0.2680(2)	0.0598(2)	0.9590(2)	2.64(3)	
N(1)	0.2975(8)	0.3694(7)	0.7333(6)	3.5(1)	
N(2)	0.1716(8)	0.2001(8)	0.6013(5)	3.3(1)	
N(3)	0.4598(7)	0.0310(7)	0.7059(6)	3.2(1)	
C(1)	0.032(1)	0.4142(9)	0.8838(8)	3.9(2)	
C(2)	0.158(1)	0.4897(10)	0.7700(9)	4.5(2)	
C(3)	0.007(1)	−0.0267(10)	0.7066(7)	3.7(2)	
C(4)	0.1160(10)	0.062(1)	0.5868(7)	3.7(2)	
C(5)	0.4178(9)	−0.1088(9)	0.9279(7)	3.3(2)	
C(6)	0.5382(9)	−0.043(1)	0.8055(8)	3.9(2)	
N(4)	0.2580(9)	0.6589(10)	0.4460(7)	4.5(2)	
N(5)	0.500(2)	0.513(2)	0.095(3)	7.9(6)	1/2
O(1)	0.152(1)	0.581(1)	0.4648(8)	7.8(2)	
O(2)	0.247(2)	0.800(2)	0.423(2)	9.0(5)	2/3
O(3)	0.379(1)	0.584(2)	0.478(1)	6.8(3)	2/3
O(4)	0.322(4)	0.711(4)	0.322(3)	9.4(9)	1/3
O(5)	0.305(5)	0.729(5)	0.490(3)	9(1)	1/3
O(6)	0.407(2)	0.475(2)	0.052(2)	6.8(5)	1/2
O(7)	0.634(3)	0.536(3)	0.009(3)	9.4(8)	1/2
O(8)	0.455(2)	0.529(2)	0.197(1)	5.8(4)	1/2
O(1w)	0.186(2)	0.361(2)	0.311(2)	7.8(5)	1/2
O(2w)	0.4870(8)	0.2439(8)	0.4023(6)	5.3(2)	

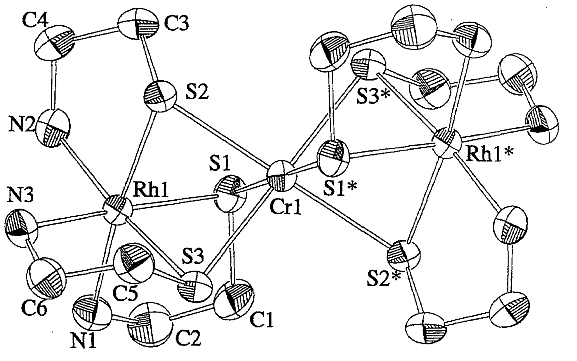

Fig. 1. Perspective view of $\Delta\Lambda$-$[Cr\{Rh(aet)_3\}_2]^{3+}$ (**1a**) with the atomic labeling scheme.

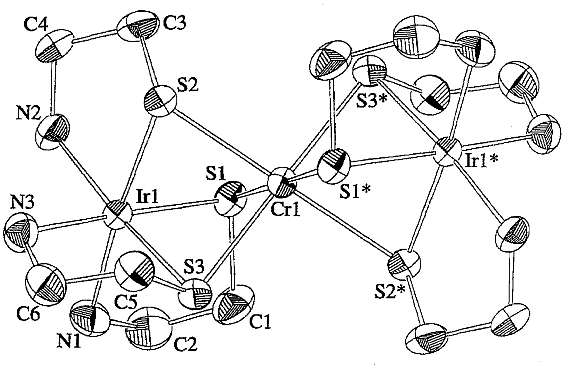

Fig. 2. Perspective view of $\Delta\Lambda$-$[Cr\{Ir(aet)_3\}_2]^{3+}$ (**2a**) with the atomic labeling scheme.

Table 4. Selected Bond Distances (Å) and Angles (Degree) for $[Cr\{Rh(aet)_3\}_2](NO_3)_3 \cdot 3H_2O$ (**1a**)

Rh(1)–Cr(1)	2.9328(2)	Rh(1)–S(1)	2.3186(8)
Rh(1)–S(2)	2.3264(8)	Rh(1)–S(3)	2.3245(8)
Rh(1)–N(1)	2.109(3)	Rh(1)–N(2)	2.106(3)
Rh(1)–N(3)	2.118(3)	Cr(1)–S(1)	2.4037(7)
Cr(1)–S(2)	2.4268(7)	Cr(1)–S(3)	2.4024(8)
S(1)–Rh(1)–S(2)	87.48(3)	S(1)–Rh(1)–S(3)	88.47(3)
S(1)–Rh(1)–N(1)	85.95(8)	S(1)–Rh(1)–N(2)	89.94(8)
S(1)–Rh(1)–N(3)	174.02(7)	S(2)–Rh(1)–S(3)	86.93(3)
S(2)–Rh(1)–N(1)	173.21(7)	S(2)–Rh(1)–N(2)	86.59(8)
S(2)–Rh(1)–N(3)	90.76(8)	S(3)–Rh(1)–N(1)	91.16(8)
S(3)–Rh(1)–N(2)	173.39(8)	S(3)–Rh(1)–N(3)	85.73(8)
N(1)–Rh(1)–N(2)	95.1(1)	N(1)–Rh(1)–N(3)	95.6(1)
N(2)–Rh(1)–N(3)	95.7(1)	S(1)–Cr(1)–S(1)^{*1}	180.0
S(1)–Cr(1)–S(2)	83.34(2)	S(1)–Cr(1)–S(2)^{*1}	96.66(2)
S(1)–Cr(1)–S(3)	84.74(3)	S(1)–Cr(1)–S(3)^{*1}	95.26(3)
S(2)–Cr(1)–S(2)^{*1}	180.0	S(2)–Cr(1)–S(3)	82.98(3)
S(2)–Cr(1)–S(3)^{*1}	97.02(3)	S(3)–Cr(1)–S(3)^{*1}	180.0
Rh(1)–S(1)–Cr(1)	76.76(2)	Rh(1)–S(2)–Cr(1)	76.16(2)
Rh(1)–S(3)–Cr(1)	76.68(2)		

*1, 2_557.

racemate, $\Delta\Delta$- and $\Lambda\Lambda$-$[Cr\{M(aet)_3\}_2]^{3+}$. The results are also supported by the facts that the molar conductivity in water and the magnetic moments at 296 K of **1b** and **2b** are in good agreement with those of **1a** and **2a**, respectively

Table 5. Selected Bond Distances (Å) and Angles (Degree) for $[\mathrm{Cr}\{\mathrm{Ir(aet)_3}\}_2](\mathrm{NO_3})_3\cdot 3\mathrm{H_2O}$ (**2a**)

Ir(1)–Cr(1)	2.9096(3)	Ir(1)–S(1)	2.328(2)
Ir(1)–S(2)	2.332(2)	Ir(1)–S(3)	2.330(2)
Ir(1)–N(1)	2.117(6)	Ir(1)–N(2)	2.106(6)
Ir(1)–N(3)	2.127(6)	Cr(1)–S(1)	2.416(2)
Cr(1)–S(2)	2.438(2)	Cr(1)–S(3)	2.408(2)
S(1)–Ir(1)–S(2)	88.40(6)	S(1)–Ir(1)–S(3)	89.24(6)
S(1)–Ir(1)–N(1)	86.2(2)	S(1)–Ir(1)–N(2)	89.9(2)
S(1)–Ir(1)–N(3)	174.7(2)	S(2)–Ir(1)–S(3)	87.70(6)
S(2)–Ir(1)–N(1)	174.4(2)	S(2)–Ir(1)–N(2)	86.5(2)
S(2)–Ir(1)–N(3)	90.1(2)	S(3)–Ir(1)–N(1)	90.8(2)
S(3)–Ir(1)–N(2)	174.2(2)	S(3)–Ir(1)–N(3)	85.7(2)
N(1)–Ir(1)–N(2)	94.9(2)	N(1)–Ir(1)–N(3)	95.2(2)
N(2)–Ir(1)–N(3)	95.1(2)	S(1)–Cr(1)–S(1)*1	180.0
S(1)–Cr(1)–S(2)	84.05(6)	S(1)–Cr(1)–S(3)	85.42(6)
S(1)–Cr(1)–S(2)*1	95.95(6)	S(1)–Cr(1)–S(3)*1	94.58(6)
S(2)–Cr(1)–S(2)*1	180.0	S(2)–Cr(1)–S(3)	83.61(6)
S(2)–Cr(1)–S(3)*1	96.39(6)	S(3)–Cr(1)–S(3)*1	180.0
Ir(1)–S(1)–Cr(1)	75.63(5)	Ir(1)–S(2)–Cr(1)	75.14(5)
Ir(1)–S(3)–Cr(1)	75.76(5)		

*1, 2_757.

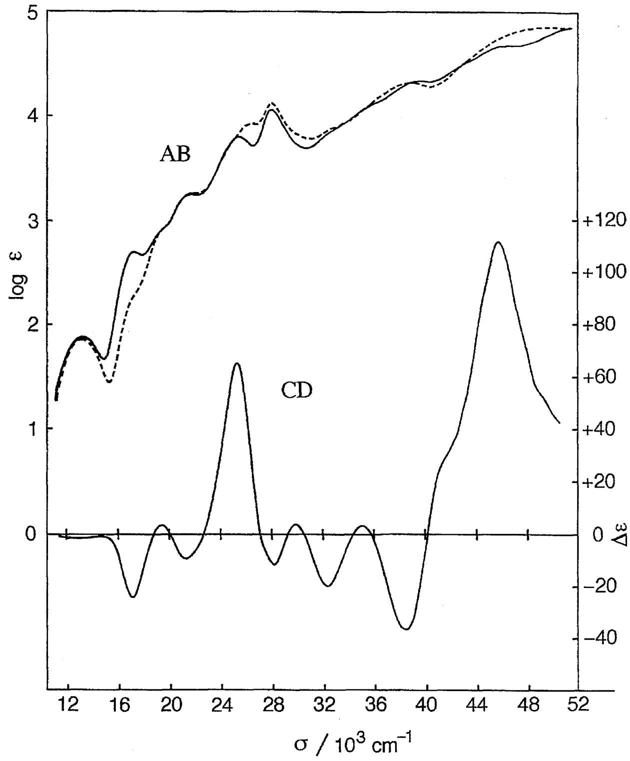

Fig. 3. Electronic absorption and CD spectra of $[\mathrm{Cr}\{\mathrm{Rh(aet)_3}\}_2]^{3+}$; $(-)^{\mathrm{CD}}_{600}$ isomer (**1b**; ——) and meso isomer (**1a**; - - -).

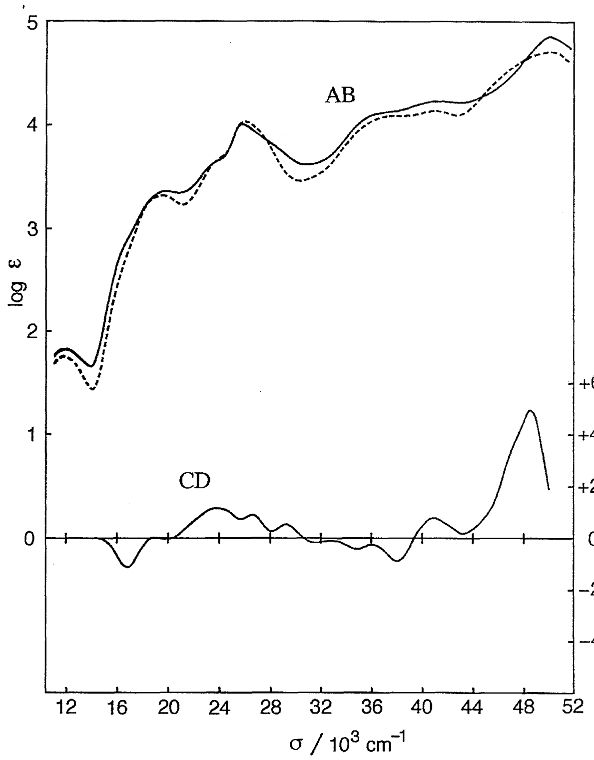

Fig. 4. Electronic absorption and CD spectra of $[\mathrm{Cr}\{\mathrm{Ir(aet)_3}\}_2]^{3+}$; $(-)^{\mathrm{CD}}_{600}$ isomer (**2b**; ——) and meso isomer (**2a**; - - -).

(Table 7).

The absorption spectra of $(-)^{\mathrm{CD}}_{600}$-$[\mathrm{Cr}\{\mathrm{M(aet)_3}\}_2]^{3+}$ ($\mathrm{M} = \mathrm{Rh^{III}}$ (**1b**) or $\mathrm{Ir^{III}}$ (**2b**)) and $\Delta\Delta$-$[\mathrm{Co}\{\mathrm{M(aet)_3}\}_2]^{3+}$ resemble each other (Figs. 3 and 4), although the absorption bands of $(-)^{\mathrm{CD}}_{600}$-**1b** or $(-)^{\mathrm{CD}}_{600}$-**2b** commonly shift to higher energy than those of $\Delta\Delta$-$[\mathrm{Co}\{\mathrm{M(aet)_3}\}_2]^{3+}$.[9,11] The characteristic intense bands in the visible and near-ultraviolet absorption band regions of the corresponding complexes, $[\mathrm{Co}\{\mathrm{M(aet)_3}\}_2]^{3+}$, are assigned as arising from the central $\mathrm{Co^{III}S_6}$ chromophore, taking account of the absorption spectral behavior of the *fac*(*S*)-$[\mathrm{M(aet)_3}]$ units in the corresponding region.[9,11] Therefore, it is assumed that the characteristic intense bands in the visible and near-ultraviolet absorption band regions ($12—30\times10^3$ cm^{-1}) of $[\mathrm{Cr}\{\mathrm{M(aet)_3}\}_2]^{3+}$ depend on the $\mathrm{Cr^{III}S_6}$ chromophore, as in the case of the $\mathrm{Co^{III}S_6}$ chromophore. In the region of $12—30\times10^3$ cm^{-1}, it is noted that the absorption bands for $[\mathrm{Cr}\{\mathrm{Ir(aet)_3}\}_2]^{3+}$ are located at a lower energy than those for $[\mathrm{Cr}\{\mathrm{Rh(aet)_3}\}_2]^{3+}$. A similar spectral behavior was also observed for $[\mathrm{Co}\{\mathrm{M(aet)_3}\}_2]^{3+}$.[9,11] Accordingly, these facts seem to reflect that the thiolato sulfur atoms in *fac*(*S*)-$[\mathrm{Ir(aet)_3}]$ possess an electron donating ability weaker than those in *fac*(*S*)-$[\mathrm{Rh(aet)_3}]$. This is supported by an X-ray crystal analysis that the Cr–S bond distances in $[\mathrm{Cr}\{\mathrm{Ir(aet)_3}\}_2]^{3+}$ are longer than those of $[\mathrm{Cr}\{\mathrm{Rh(aet)_3}\}_2]^{3+}$. The CD spectral behavior of $(-)^{\mathrm{CD}}_{600}$-**1b** is in agreement with that of $\Delta\Delta$-$[\mathrm{Co}\{\mathrm{Rh(aet)_3}\}_2]^{3+}$ over the whole region,[9] considering the absorption spectral shift. Accordingly, it seems to be assigned that $(-)^{\mathrm{CD}}_{600}$-**1b** and $(+)^{\mathrm{CD}}_{600}$-**1b** are $\Delta\Delta$- and $\Lambda\Lambda$-$[\mathrm{Cr}\{\mathrm{Rh(aet)_3}\}_2]^{3+}$, respectively. It is also assigned quite similarly that $(-)^{\mathrm{CD}}_{600}$-**2b** and $(+)^{\mathrm{CD}}_{600}$-**2b** are $\Delta\Delta$- and $\Lambda\Lambda$-$[\mathrm{Cr}\{\mathrm{Ir(aet)_3}\}_2]^{3+}$, respectively, by comparing with corresponding $\Delta\Delta$-$[\mathrm{Co}\{\mathrm{Ir(aet)_3}\}_2]^{3+}$ complex.[11]

Syntheses and Reactivity. The reaction of *fac*(*S*)-$[\mathrm{M(aet)_3}]$ ($\mathrm{M}=\mathrm{Rh^{III}}, \mathrm{Ir^{III}}$) with a large excess of chromium(III) nitrate in water at 60 °C gave *meso*- and *rac*-$[\mathrm{Cr}\{\mathrm{M(aet)_3}\}_2]^{3+}$,

Table 6. Electronic Absorption and CD Spectral Data of $[\mathrm{Cr}\{\mathrm{M(aet)_3}\}_2]^{3+}$

Complex ion	Absorption maxima $\sigma/10^3\ \mathrm{cm^{-1}}$ ($\log\varepsilon/\mathrm{mol^{-1}\ dm^3\ cm^{-1}}$)	CD extrema $\sigma/10^3\ \mathrm{cm^{-1}}$ ($\Delta\varepsilon/\mathrm{mol^{-1}\ dm^3\ cm^{-1}}$)
$\Delta\Lambda$-$[\mathrm{Cr}\{\mathrm{Rh(aet)_3}\}_2]^{3+}$ (**1a**)	13.09 (1.86)	
	17.5 (2.3sh)	
	22.0 (3.3sh)	
	26.53 (3.93)	
	28.01 (4.12)	
	38.91 (4.32)	
	49.75 (4.85)	
$(-)^{\mathrm{CD}}_{600}$-$\Delta\Delta$-$[\mathrm{Cr}\{\mathrm{Rh(aet)_3}\}_2]^{3+}$ (($(-)^{\mathrm{CD}}_{600}$-$\Delta\Delta$-**1b**)	13.19 (1.90)	13.07 (−1.4)
	17.21 (2.71)	17.09 (−24.1)
	21.9 (3.3sh)	19.38 (+3.5)
	25.38 (3.81)	21.23 (−9.3)
	28.01 (4.07)	25.25 (+65.6)
	39.53 (4.34)	28.17 (−11.7)
	46.5 (4.7sh)	29.85 (+3.7)
		32.26 (−20.0)
		35.09 (+3.1)
		38.46 (−36.7)
		45.66 (+112.5)
$\Delta\Lambda$-$[\mathrm{Cr}\{\mathrm{Ir(aet)_3}\}_2]^{3+}$ (**2a**)	11.78 (1.75)	
	16.3 (2.6sh)	
	19.61 (3.31)	
	23.9 (3.7sh)	
	25.97 (4.02)	
	27.8 (3.8sh)	
	37.5 (4.1sh)	
	40.98 (4.13)	
	50.00 (4.71)	
$(-)^{\mathrm{CD}}_{600}$-$\Delta\Delta$-$[\mathrm{Cr}\{\mathrm{Ir(aet)_3}\}_2]^{3+}$ (($(-)^{\mathrm{CD}}_{600}$-$\Delta\Delta$-**2b**)	11.99 (1.84)	16.81 (−11.2)
	16.6 (2.8sh)	18.90 (+0.2)
	19.80 (3.36)	19.84 (−0.3)
	23.7 (3.6sh)	23.75 (+11.5)
	25.84 (4.00)	26.60 (+8.9)
	28.6 (3.8sh)	29.24 (+5.3)
	36.5 (4.1sh)	31.55 (−1.6)
	41.32 (4.23)	34.84 (−4.1)
	50.00 (4.86)	38.02 (−8.7)
		40.82 (+8.0)
		48.54 (+49.8)

sh denotes a shoulder.

Table 7. Molar Conductivity ($\Lambda_\mathrm{m}/\Omega^{-1}\ \mathrm{cm^2\ mol^{-1}}$)[a] and Magnetic Moments (μ_eff/B.M.)[b] of $[\mathrm{Cr}\{\mathrm{M(aet)_3}\}_2]^{3+}$

		Λ_m	μ_eff
$\Delta\Lambda$-$[\mathrm{Cr}\{\mathrm{Rh(aet)_3}\}_2]^{3+}$	(**1a**)	352	3.95
$\Delta\Delta/\Lambda\Lambda$-$[\mathrm{Cr}\{\mathrm{Rh(aet)_3}\}_2]^{3+}$	(**1b**)	377	3.87
$\Delta\Lambda$-$[\mathrm{Cr}\{\mathrm{Ir(aet)_3}\}_2]^{3+}$	(**2a**)	355	3.77
$\Delta\Delta/\Lambda\Lambda$-$[\mathrm{Cr}\{\mathrm{Ir(aet)_3}\}_2]^{3+}$	(**2b**)	369	3.76

a) in water. b) at 296 K.

whose formation ratio was ca. 1 : 1. The trinuclear MCrM complexes, in which the Cr(III) ion is bound by the six S donor atoms and incorporated in the S-bridged polynuclear structure, were hardly formed by a reaction using an equivalent amount of chromium(III) nitrate or by a reaction at room temperature. These are in contrast to the fact that the corresponding complexes, $[\mathrm{Co}\{\mathrm{M(aet)_3}\}_2]^{3+}$, were formed by the reaction of *fac*(*S*)-$[\mathrm{M(aet)_3}]$ with an equivalent amount of $[\mathrm{CoCl(NH_3)_5}]^{2+}$ or Co(II) at room temperature.[9,11] In Cr(III) complexes with L-cysteinate (L-cys), $[\mathrm{Cr}(\text{L-cys-}N,O,S)_2]^-$[13—15,22,28] and $[\mathrm{Cr}(\text{L-Hcys-}N,O)_3]$[29] have been obtained but $[\mathrm{Cr}(\text{L-Hcys-}N,S)_3]$ has not. These are significantly different from those for the Co(III) and Rh(III) complexes with L-cysteinate, in which [M(L-Hcys-*N*,*S*)$_3$] is easily formed.[9,30,31] Moreover, the central Cr(III) ion in the trinuclear complex $[Cr\{Cr(SCH_2CH_2O)_3\}_2]^{3-}$, in which the terminal units have both of the facial(O) or facial(S) coordination sites, has been bridged by alkoxide oxygen atoms.[27] Accordingly, it seems to be indicated that the difficulty concerning the formation of the MCrM trinuclear complexes should be due to the weak affinity of the Cr(III) ion toward the S atoms, since the Cr(III) complexes prefer an O coordination mode to an S one.

When each isomer of the MCrM trinuclear complexes under an excess amount of the Cr(III) ion was stirred for a few hours in warm water, both the meso and racemic isomers were found by a column chromatographic method. A similar geometrical isomerization was recognized in trinuclear MM′M ($M' = Co^{III}$, Ni^{II}) complexes.[11,12] Further, although the Cr–S bond cleavage is apt to occur in acid condition, we had to handle the reaction under acidic conditions because the neutralization caused the precipitation of Cr hydroxide. In the synthesis of IrCrIr complexes under acidic conditions, the *fac*(*S*)-[Ir(aet)$_3$] unit would be oxidized by acid and this oxidized complex is assigned to the IrIr dinuclear complex with a bridging disulfide bond, $[Ir_2(aet)_4(cysta)]^{2+}$ (cysta=cystamine).[32] For the corresponding RhCrRh synthesis, in which *fac*(*S*)-[Rh(aet)$_3$] is oxidized more hardly than *fac*(*S*)-[Ir(aet)$_3$], a similar reaction may not form a dinuclear complex with a bridging disulfide, although the compound, which showed a similar absorption spectrum to that by treating *fac*(*S*)-[Rh(aet)$_3$] with acid, was also obtained. Therefore, the formation of MCrM complexes are highly dependent on the reaction conditions.

The IrCrIr trinuclear complexes were formed and decomposed more easily than the corresponding RhCrRh complexes. These facts suggest that the Cr–S bonds in the IrCrIr complex are weaker than those in the RhCrRh complex, presumably because of the stronger Ir–S bonds than the Rh–S ones. Similar results were observed for the MCoM trinuclear complexes.[9,11] In *meso*- and *rac*-$[Cr\{M(aet)_3\}_2]^{3+}$, they are fairly stable in water at room temperature, and their absorption spectra change only slightly with time. However, the more the temperature or acidity increases, the greater does the degree of the changes with time become. Since the meso and racemic isomers exhibit a quite similar stability to each other, plots of the changes with times of *meso*-$[Cr\{Ir(aet)_3\}_2]^{3+}$, which were determined by the column chromatographic technique and the absorption spectral measurements, under acidic condition of 1 mol dm^{-3} HCl solution are shown in Fig. 5. The existences of the IrCrIr trinuclear complexes gradually decrease, while those of the IrIr dinuclear complex, $[Ir_2(aet)_4(cysta)]^{2+}$, increase more complicately. The spectral changes in $[Cr\{Ir(aet)_3\}_2]^{3+}$ involve mainly a decrease of the intense bands, which are assigned as arising from the central $Cr^{III}S_6$ chromophore. The IrCrIr complex exhibits its absorption peak at 385 nm and the IrIr complex also shows a high absorbance at its wavelength (Fig. 4).[32] The absorbances calculated from the ratio of the IrCrIr and the IrIr complexes, which were determined by column chromatography, coincide well with those measured from the reaction mixture at 385 nm (Fig. 5). These facts mean that the unidentified compounds exhibit no significant absorbances in this region, indicating that they will involve the mononuclear Ir and Cr complexes or ions. Although systematic changes are not implied completely, further, the plots of log(existence) vs. time for the IrCrIr trinuclear and IrIr dinuclear complexes seem to indicate that although the IrCrIr trinuclear complex is gradually decomposed, its decomposition is inhibited by an increase of the Cr(III) ion (Fig. 5). Since the IrIr complex is formed in spite of the absence of the IrCrIr trinuclear complex, the IrIr complex seems to be rearranged from the decomposition compounds.

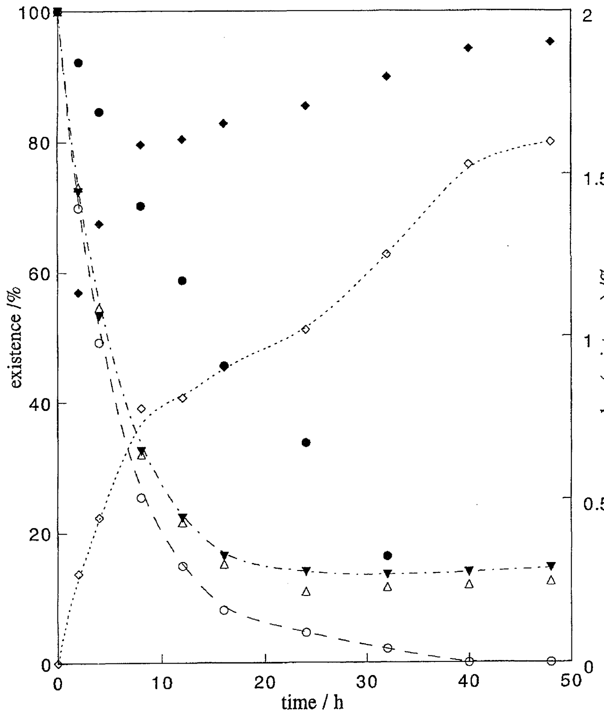

Fig. 5. Changes with times of *meso*-$[Cr\{Ir(aet)_3\}_2]^{3+}$; chromatographic technique, $[Cr\{Ir(aet)_3\}_2]^{3+}$ (○) and $[Ir_2(aet)_4(cysta)]^{2+}$ (◇); absorbance changes at 385 nm, calculation values of $\varepsilon([Cr\{Ir(aet)_3\}_2]^{3+})+\varepsilon([Ir_2(aet)_4(cysta)]^{2+})$ (▼) and measurements (△). Plots of log (existence) vs. time; $[Cr\{Ir(aet)_3\}_2]^{3+}$ (●) and $[Ir_2(aet)_4(cysta)]^{2+}$ (◆).

Electrochemistry. Electrochemical studies were performed for *meso*-$[Cr^{III}\{M(aet)_3\}_2]^{3+}$ ($M = Rh^{III}$ (**1**), Ir^{III} (**2**)) in 0.1 mol dm^{-3} Na_2SO_4 aqueous solutions. As shown in Fig. 6, the cyclic voltammograms for both **1a** and **2a** display a reversible redox couple at a positive potential region and an irreversible reduction wave at a negative region. It seems to be indicated that the reversible redox couple ($E^{\circ\prime} = +1.01$ V; $E_{pa} = +1.05$ V; $E_{pc} = +0.97$ V) for the $Rh^{III}Cr^{III}Rh^{III}$ complex involves the terminal Rh(IV)/Rh(III) redox process, because a similar redox couple appeared at almost the same positive region as that of the $Rh^{III}Co^{III}Rh^{III}$ complex ($E^{\circ\prime} = +1.01$ V).[11] Similarly, the reversible redox couple ($E^{\circ\prime} = +0.64$ V; $E_{pa} = +0.68$ V; $E_{pc} = +0.60$ V) for the $Ir^{III}Cr^{III}Ir^{III}$ complex would involve the terminal Ir(IV)/Ir(III) redox process, because a similar redox couple appeared at almost a similar

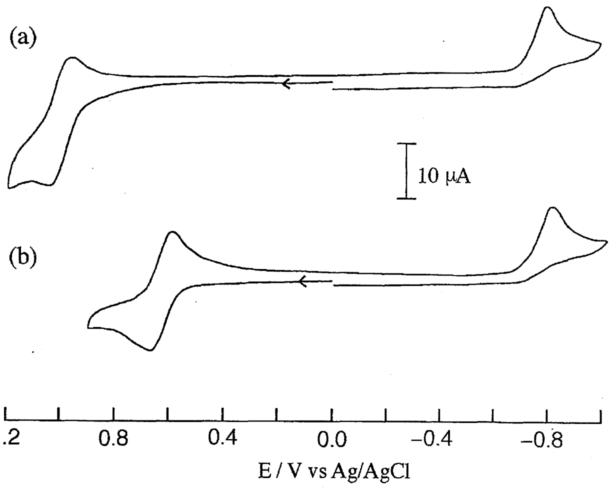

Fig. 6. Cyclic voltammograms of $[Cr\{M(aet)_3\}_2]^{3+}$; (a) M = Rh and (b) M = Ir; scan rate 100 mV s^{-1}; in 0.1 mol dm^{-3} Na_2SO_4 aqueous solution.

positive region to the $Ir^{III}Co^{III}Ir^{III}$ complex ($E°' = +0.73$ V), although the Cr(III) complex appeared at 0.09 V more negative than the Co(III) complex.[11] Therefore, the $Ir^{III}Cr^{III}Ir^{III}$ complex is generally oxidized more easily than the $Rh^{III}Cr^{III}Rh^{III}$ complex, as it is observed in the $MCo^{III}M$ complexes.

The irreversible reduction waves ($E_{pc} = -0.86$ V) for $[Cr^{III}\{Rh(aet)_3\}_2]^{3+}$ appear at almost the same potential as that for ($E_{pc} = -0.85$ V) for the $Ir^{III}Cr^{III}Ir^{III}$ complex. Since it has been known that the Rh(III)/Rh(II) and Ir(III)/Ir(II) redox process does not occur in the potential region of +1.1—−1.1 V for the $Rh^{III}Co^{III}Rh^{III}$ and $Ir^{III}Co^{III}Ir^{III}$ complexes,[11] the irreversible reduction waves are probably the central Cr(III)/Cr(II) reduction process and are implied by the decomposition of the complexes. On the other hand, the Co(III)/Co(II) redox couple ($E°' = -0.23$ V) for the $Ir^{III}Co^{III}Ir^{III}$ complex appears at 0.13 V more positive than that ($E°' = -0.36$ V) for the $Rh^{III}Co^{III}Rh^{III}$ complex, indicating that the central Co(III) is made easier to reduce by the terminal *fac*(*S*)-$[Ir(aet)_3]$ units than the *fac*(*S*)-$[Rh(aet)_3]$ units.[11] Accordingly, the electrochemical behavior of the central Cr(III) ion in the $MCr^{III}M$ complexes is significantly different from that of the Co(III) ion in the $MCo^{III}M$ ones; that is, it seems to be indicated that the central Cr(III) in the $MCr^{III}M$ complex is hardly reduced and the trinuclear structure no longer exists when it is reduced. This means that in the trinuclear MM′M (M = Rh^{III}, Ir^{III}; M′ = Cr^{III}, Co^{III}) complexes, the Ir–S bonds are stronger than the Rh–S bonds and the Co–S bonds are stronger than the Cr–S bonds, as indicated by their stereochemical and spectrochemical behavior. Therefore, the present electrochemical results also suggest that the M–S bond strengths are the factor of the electrochemical differences of the complexes.

This work was supported by a Grant-in-Aid for Scientific Research No. 07454172 from the Ministry of Education, Science and Culture.

References

1) D. H. Busch and D. C. Jicha, *Inorg. Chem.*, **1**, 884 (1962).

2) G. R. Brubaker and B. E. Douglas, *Inorg. Chem.*, **6**, 1562 (1967).

3) R. E. DeSimome, T. Ontko, L. Wardman, and E. L. Blinn, *Inorg. Chem.*, **14**, 1313 (1975).

4) E. L. Blinn, P. Butler, K. M. Chapman, and S. Harris, *Inorg. Chim. Acta*, **24**, 139 (1977).

5) G. R. Brubaker, M. G. Henk, and D. W. Johnson, *Inorg. Chim. Acta*, **100**, 201 (1985).

6) M. J. Heeg, E. L. Blinn, and E. Deutsch, *Inorg. Chem.*, **24**, 1118 (1985).

7) D. W. Johnson and T. R. Brewer, *Inorg. Chim. Acta*, **154**, 221 (1988).

8) T. Konno, S. Aizawa, and J. Hidaka, *Bull. Chem. Soc. Jpn.*, **62**, 585 (1989).

9) T. Konno, S. Aizawa, K. Okamoto, and J. Hidaka, *Bull. Chem. Soc. Jpn.*, **63**, 792 (1990).

10) T. Konno, K. Okamoto, and J. Hidaka, *Acta Crystallogr., Sect. C*, **C49**, 222 (1993).

11) T. Konno, K. Nakamura, K. Okamoto, and J. Hidaka, *Bull. Chem. Soc. Jpn.*, **66**, 2582 (1993).

12) T. Konno and K. Okamoto, *Bull. Chem. Soc. Jpn.*, **68**, 610 (1995).

13) J. A. Cooper, L. F. Blackwell, and P. D. Buckley, *Inorg. Chim. Acta*, **92**, 23 (1984).

14) P. O'Brien, J. D. P. de Jesus, and T. M. Santos, *Inorg. Chim. Acta*, **131**, 5 (1987).

15) T. M. Santos, J. P. de Jesus, and P. O'Brien, *Polyhedron*, **11**, 1687 (1992).

16) M. Kita, K. Yamanari, and Y. Shimura, *Bull. Chem. Soc. Jpn.*, **56**, 3272 (1983).

17) T. Konno, K. Okamoto, and J. Hidaka, *Inorg. Chem.*, **33**, 538 (1994).

18) "teXsan. Molecular Structure Corporation. Single Crystal Structure Analysis Software. Version 1.7," MSC, 3200 Research Forest Drive, The Woodlands, TX 77381, USA (1995).

19) Lists of structure factors, hydrogen atoms coordinates, bond distances and angles, and anisotropic thermal parameters for non-hydrogen atoms are deposited as Document No. 71014 at the Office of the Editor of Bull. Chem. Soc. Jpn.

20) A. C. Villa, A. G. Manfredotti, C. Guastini, and M. Nardelli, *Acta Crystallogr., Sect. B*, **B30**, 2788 (1974).

21) K. Okamoto, M. Matsumoto, Y. Miyashita, N. Sakagami, J. Hidaka, and T. Konno, *Inorg. Chim. Acta*, **260**, 17 (1997).

22) P. de Meester, D. J. Hodgson, H. C. Freeman, and C. J. Moore, *Inorg. Chem.*, **16**, 1494 (1977).

23) C. Stein, S. Bouma, J. Carlson, C. Cornelins, J. Maeda, C. Weschler, E. Deutsch, and K. O. Hodgson, *Inorg. Chem.*, **15**, 1183 (1976).

24) M. Mitsumi, H. Okawa, H. Sakiyama, M. Ohba, N. Matsumoto, T. Kurisaki, and H. Wakita, *J. Chem. Soc., Dalton Trans.*, **1993**, 2991.

25) R. C. Elder, L. R. Florian, R. E. Lake, and A. M. Yacynych, *Inorg. Chem.*, **12**, 2690 (1973).

26) P. de Meester and D. J. Hodgson, *J. Chem. Soc., Chem. Commun.*, **1976**, 280; P. de Meester and D. J. Hodgson, *J. Chem. Soc., Dalton Trans.*, **1977**, 1604.

27) J. R. Nicholson, R. Mang, J. C. Hoffman, G. Christou, H. Chang, and D. N. Hendrickson, *J. Chem. Soc., Chem. Commun.*,

1985, 1781; J. R. Nicholson, G. Christou, R. Wang, J. C. Hoffman, H. Chang, and D. N. Hendrickson, *Polyhedron*, **10**, 2255 (1991).

28) M. Abdullah, J. Barrett, and P. O'Brien, *J. Chem. Soc., Dalton Trans.*, **1985**, 2085.

29) M. S. El-Shahawi, *Spectrochim. Acta, Part A*, **51A**, 161 (1995).

30) M. P. Schubert, *J. Am. Chem. Soc.*, **55**, 3336 (1933).

31) K. Okamoto, S. Aizawa, T. Konno, H. Einaga, and J. Hidaka, *Bull. Chem. Soc. Jpn.*, **59**, 3859 (1986).

32) T. Konno, Y. Miyashita, and K. Okamoto, *Chem. Lett.*, **1997**, 85.